Asian Journal of Chemistry; Vol. 38, No. 3 (2026), 636-642
ASIAN JOURNAL OF CHEMISTRY
https://doi.org/10.14233/ajchem.2026.35199

Ultrasound Assisted Synthesis, X-Ray Diffraction, DFT and Antibacterial Studies of Naphthalenyl-hydrazinyl- and Quinazolinyl-thiazole Derivatives

SWATI GOSWAMI and R.P. CHAUDHARY*

Department of Chemistry, Sant Longowal Institute of Engineering & Technology, Longowal-148106, India

*Corresponding author: E-mail: rpchaudhary65@gmail.com

Received: 6 November 2025 *Accepted*: 29 December 2025 *Published online*: 6 March 2026 AJC-22282

Naphthalenyl-hydrazinecarbothioamides **2**, obtained from reaction of 1-tetralones (**1**) and thiosemicarbazide, on condensation with ethyl bromopyruvate under ultrasonic conditions furnished thiazole-4-carboxylates (**3**). Ultrasound assisted synthesis of quinazoline-thiazole hybrids **5** was achieved from reaction of quinazolinyl-thiones (**4**) with 3-chloropentane-2,4-dione. The structural elucidation of novel compounds was determined with the help of spectral techniques. X-ray crystallographic studies (SCXRD) of single crystal of thiazole-4-carboxylate **3a** along with supramolecular interactions in crystal packing were also reported. *In silico* studies of regioisomers **5** and **6** were computed to correlate the experimental and theoretical spectral data. Compound **5a** has shown good activity against *S. aureus* (MIC 25 μg/mL) and *E. coli* (50 μg/mL) bacterial strains.

Keywords: Thiazole-4-carboxylate, Quinazoline-thiazole, X-ray diffraction, DFT, Antibacterial activity.

INTRODUCTION

Among heterocycles, thiazole ring is an interesting architecture, which induce sigma and pi-interactions with receptors moieties that are helpful in drug designing [1,2]. In past few decades, this moiety allured chemists due its presence in wide library of natural and synthetic compounds with diverse biological profiles [2,3]. Detection of thiazole nucleus in natural products notably, vitamin B1 (thiamine) and penicillin fascinated the chemists for exploration of its pharmaceutical potential [3-5]. Therefore, thaizole derivatives gain significant attention due to their biological pursuit as anticancer [6], antiviral [7], antibacterial [8,9], antifungal [10], antitubercular [11], anti-inflammatory [12], *etc*. activities. Several antiparasitic drugs, such as nitazoxanide and aminotrozole, incorporate the thiazole ring [13], which is also present in clinically approved agents used to treat peptic ulcers, target helminth-specific mitochondrial enzymes and manage cancer and HIV infection [14,15]. Furthermore, introduction of carboxylate group in thiazole ring enhances their biological potential [16,17].

Similarly, quinazoline moiety is also found in many natural products of potential biological activities. Fusion of this nucleus with other biological active moieties portray synergistic activity profile [18-20]. Thus, based on these facts, in this work, two new quinazolinyl-thiazole hybrids were synthesized under ultrasonication and their antibacterial activity was investigated.

In recent years, computational methods like DFT studies [21-23] have also become an important tool for a synthetic chemist by extending support to the determination of structural parameters by comparison of experimental and theoretical models. Consequently, it has become a preferred method for studying molecular stability, frontier molecular orbitals, and spectroscopic characteristics of diverse chemical compounds [24,25]. Thus, in this work, DFT studies were also performed on a pair of regioisomers **5a** and **6a**, which offers an additional support for validation of the assigned structure.

EXPERIMENTAL

Reagents used in this study were procured from the commercial sources and utilised without purification. BRUKER AVANCE Neo 500 MHz spectrometer was utilised for recording proton and decoupled carbon NMR in $CDCl_3$ and DMSO-d_6 solvents. Chemical shifts were measured in parts per million (ppm) with reference to tetramethyl silane. Q-TOF Micro mass Waters, LC-MS SCIEX Triple TOF 5600, 5600+/ SCIEX equipped with electrospray ionisation (ESI-MS) and chemical ionisation (CI) were engaged for the mass analysis.

FTIR spectra were scanned on a Perkin-Elmer (RX) spectrophotometer in the 4000-400 cm^{-1} range using KBr pellet method. Ultrasonication experiments were conducted on Cole Parmar CPX500 ultrasonicator (20 KHz, 500 Watt). Melting points were detected using LABTRONICS, India, Model LT-115 melting point apparatus.

Synthesis of hydrazinecarbothioamide (2): Thiosemicarbazone derivatives of 1-tetralone and 6-methoxy-1-tetralone, **2a** and **2b** were synthesized by the reported method [26]. Compound **2a** was obtained as white crystalline solid; yield 82%; m.p.: 200-202 ºC (Lit. m.p.: 202-206 ºC) and compound **2b** was brown solid; yield 81%; m.p.: 195-196 ºC (Lit. m.p.: 198-200 ºC).

Synthesis of thiazole-4-carboxylate (3): A mixture of hydrazinecarbothioamide (**2**, 0.438 g, 2.0 mmol) and ethyl bromopyruvate (0.39 g, 2.0 mmol) in 10 mL ethanol was stirred under ultrasonic condition. After pouring the reaction mixture in ice water, solid product was obtained. Filtered the solid and recystallised from ethanol to procure compound **3a** as light-yellow needle-shaped solid product. Similarly, compound **3b** was synthesised from hydrazine carbothiamide **2b** (**Scheme-I**).

Ethyl 2-(2-(3,4-dihydronaphthalen-1(2*H*)-ylidene)-hydrazinyl)thiazole-4-carboxylate (3a): Light yellow; yield: 72%; m.p.: 194-196 ºC. IR (KBr, ν_{max}, cm^{-1}): 3206 (NH), 1702 (C=O), 1642 (C=N); ^{1}H NMR (400 MHz, DMSO-d_6, δ ppm): 1.30–1.34 (t, 3H, CH_3, J = 7.16 Hz), 1.84-1.90 (m, 2H, CH_2), 2.64-2.69 (t, 2H, CH_2, J = 6.44 Hz), 2.73-2.76 (t, 2H, CH_2, J = 5.92 Hz), 4.23-4.30 (q, 2H, CH_2, J = 6.5 Hz), 7.14-7.17 (m, 1H, C_6H_5), 7.20-7.25 (m, 2H, C_6H_5), 7.69 (s, 1H, CH of thiazole ring), 7.94-8.0 (m, 1H, C_6H_5), 11.39 (br, 1H, NH); MS, *m/z* 316.1 ($M+H^+$, 100%). Anal. calcd. (found) % for $C_{16}H_{17}N_3O_2S$: C, 70.04 (60.93); H, 5.62 (5.43); N, 13.58 (13.32); S, 10.34 (10.17).

Ethyl 2-(2-(6-methoxy-3,4-dihydronaphthalen-1(2*H*)-ylidene)hydrazinyl)thiazole-4-carboxylate (3b): Light orange; yield 69%; m.p.: 208-210 ºC. IR (KBr, ν_{max}, cm^{-1}): 3208 (NH), 1692 (C=O), 1638 (C=N). ^{1}H NMR (400 MHz, DMSO-d_6, δ ppm): 1.29-1.41 (t, 3H, CH_3, J = 7.08 Hz), 1.84-1.87 (m, 2H, CH_2), 2.62-2.66 (t, 2H, CH_2, J = 5.88 Hz), 2.71-2.74 (t, 2H, CH_2, J = 6.48 Hz), 3.78 (s, 3H, OCH_3), 4.23-4.28 (q, 2H, CH_2, J = 6.5 Hz), 6.70-6.81 (m, 2H, C_6H_5), 7.66 (s, 1H, CH of thiazole ring), 7.89-7.93 (m, 1H, C_6H_5), 11.32 (br, 1H, NH). Anal. calcd. (found) %for $C_{17}H_{19}N_3O_3S$: C, 59.34 (59.11); H, 5.72 (5.54); N, 12.29 (12.17); S, 9.34 (9.28).

Synthesis of thiones (4): Thiones **4a** and **4b** were synthesised from refluxing an equimolar mixture of 1-tetralone/6-methoxy-1-tetralone, benzaldehyde and thiourea in alc. KOH (1.0 g KOH + 15 mL ethanol) by the reported procedure [27] (**Scheme-II**).

4-Phenyl-3,4,5,6-tetrahydrobenzo[*h*]quinazoline-2(1*H*)-thione (4a): White crystalline solid, yield 75%; m.p.: 238-40 ºC (Lit. m.p.: 242-44 ºC): Mass (EI): *m/z* 292 (M^+, 62%), 215 (M^+-C_6H_5, 100%).

8-Methoxy-4-phenyl-3,4,5,6-tetrahydrobenzo[*h*]quinazoline-2(1*H*)-thione (4b): White crystalline solid, yield 72%; m.p.: 264-65 ºC (Lit. m.p.: 265-66 ºC).

Synthesis of regioisomers 5 or 6: A mixture of thione **4a** (0.28 g, 1.0 mmol), 3-chloropentane-2,4-dione (0.134 g, 1.0 mmol) and Et_3N (0.56 mL, 4.0 mmol) in dry DMF (6.0 mL) was stirred under ultrasonic condition for 10-15 min. The separated solid was filtered and washed with ethanol. Recrystallisation from ethanol: DMF (3:1) mixture furnished white crystalline solid **5a** or **6a**. Similarly, **5b** or **6b** were also synthesized.

1-(9-Methyl-7-phenyl-5,7-dihydro-6*H*-benzo[*h*]thiazolo[2,3-*b*]quinazoline-10yl)ethan-1-one (5a): White crystalline solid, yield: 76%; m.p.: 180-82 ºC: IR (KBr, ν_{max}, cm^{-1}): 1669 (C=O), 1636 (C=N), 1586 (C=C); ^{1}H NMR (500 MHz, DMSO-d_6, δ ppm): 2.02-2.09 (1H, m, CH_2), 2.13-2.2 (1H, m, CH_2), 2.31 (3H, s, CH_3), 2.32 (3H, s, $COCH_3$), 2.61-2.67 (1H, m, CH_2), 2.77-2.84 (1H, m, CH_2), 5.61 (1H, s, H_A), 7.04 (1H, d, C_6H_5, J = 7.3 Hz), 7.15 (1H, t, C_6H_5, J = 7.3 Hz), 7.23 (1H, d, C_6H_5, J = 7.6 Hz), 7.27-7.34 (5H, m, C_6H_5), 7.9 (1H, d,

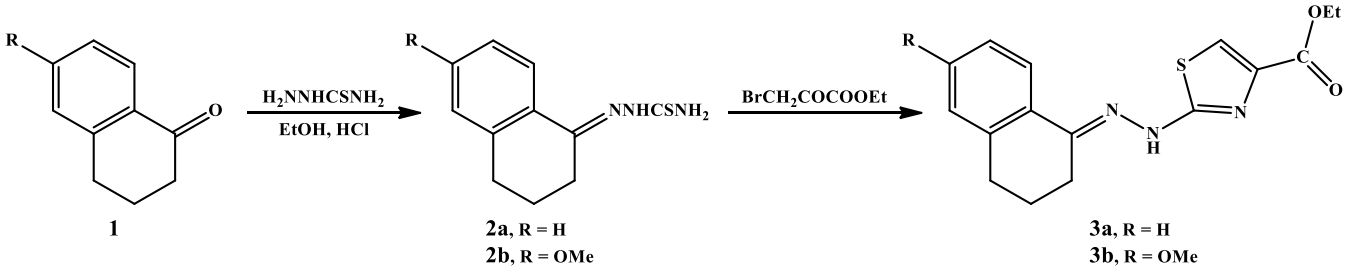

Scheme-I: Synthetic route of thiazole-4-carboxylate derivatives (**3a-b**) from 1-tetralone (**1**)

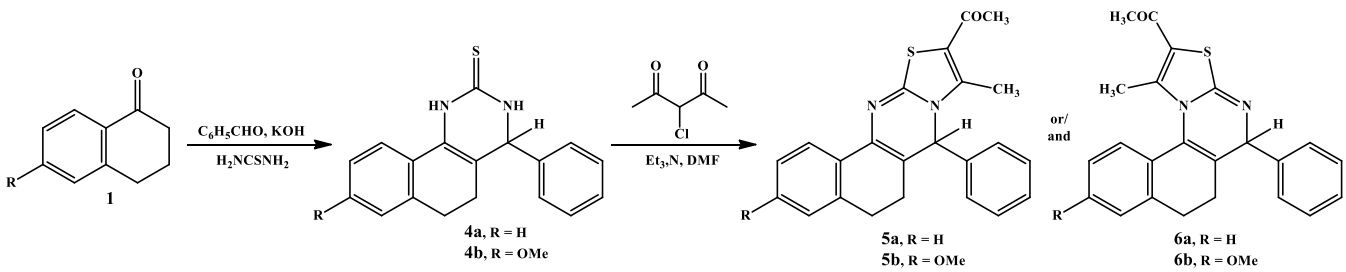

Scheme-II: Synthesis of thiazolo[2,3-*b*]quinazoline derivatives

C_6H_5, *J* = 7.3 Hz); ^{13}C NMR (125 MHz, $CDCl_3$, δ ppm): 189.4 (C=O), 158.6 (C=N), 144.5, 141.2, 135.2, 133.7, 133.1, 129.2, 128.8, 127.4, 127, 126.5, 126.4, 123.3, 112.9, 110.2, 62.9, 30.2, 27.7, 25.1, 13.6. Mass (EI): *m/z* 372 (M^+, 15%), 295 (M^+-C_6H_5, 100%).

1-(3-Methoxy-9-methyl-7-phenyl-5,7-dihydro-6*H*-benzo[*h*]thiazolo[2,3-*b*]quinazoline-10yl)ethan-1-one (5b): White crystals, yield: 72%; m.p.: 258-60 ºC: IR (KBr, ν_{max}, cm^{-1}): 1672 (C=O), 1628 (C=N), 1578 (C=C); ^{1}H NMR (500 MHz, $CDCl_3$, δ ppm): 2.04-2.11 (1H, m, CH_2), 2.15-2.21 (1H, m, CH_2), 2.35 (3H, s, CH_3), 2.36 (3H, s, $COCH_3$), 2.66-2.69 (1H, m, CH_2), 2.8-2.86 (1H, m, CH_2), 3.85 (3H, s, OCH_3), 5.75 (1H, s, H_A), 7.14 (1H, s, C_6H_5), 7.25 (1H, d, C_6H_5, *J* = 7.8 Hz), 7.38 (1H, d, C_6H_5, *J* = 7.5 Hz), 7.37-7.44 (5H, m, C_6H_5); ^{13}C NMR (125 MHz, $CDCl_3$, δ ppm): 188.6 (C=O), 156.4 (C=N), 143.5, 142.3, 137.6, 134.3, 132.4, 128.6, 128.3, 126.2, 127, 126, 125.3, 122.4, 114.6, 109.3, 63.6, 32.2, 26.5, 25, 15.7. Mass (LC-MS): *m/z* 403 (M^++H) 402 (M^++H-1), 401 (M^++H-2).

RESULTS AND DISCUSSION

Hydrazinecarbothioamides **2** were obtained from condensation of compound **1** with thiosemicarbazide in ethanol containing a few drops of conc. HCl under stirring conditions [26]. Reaction of compound **2** with ethyl bromopyruvate in ethanol under ultrasonic conditions for 15 min furnished thiazole-4-carboxylates **3** (**Scheme-I**). The IR spectrum of compound **3a** showed peak at 1702 cm^{-1} due to C=O of ester group. ^{1}H NMR spectrum of **3a** displayed a triplet of three protons at δ 1.32 ppm (*J* = 7.16 Hz) due to methyl group and a quartet of two protons at δ 4.26 ppm (*J* = 6.5 Hz) due to CH_2 of ester group. The presence of one proton singlet at δ 7.69 ppm is attributed to methine proton (=CH) of thiazole ring. The mass spectrum of compound **3a** showed the $[M+H]^+$ peak at *m/z* 316.1 (100%). The structure of compound **3b** was similarly established by elemental analysis and spectral (IR and NMR) data. The structure of compound **3a** is also confirmed by single crystal X- ray diffraction studies.

This study also reports the synthesis of thiazolo[2,3-*b*]-quinazoline derivatives **5** or/and **6**. The formation of regioisomers depends upon the orientation of cyclisation, which in fact, was established by spectral and DFT methods. Condensation of 1-tetralone with benzaldehyde and thiourea in alcoholic KOH furnished thione **4a**, which was characterised by comparing its melting point with the literature [27]. The thione **4**, on condensation with 3-chloropentane-2,4-dione in triethylamine and anhydrous ethanol under ultrasonic conditions for 15-20 min produced thiazolo[2,3-*b*]quinazoline derivatives **5** or **6** or a mixture of both. The plausible mechanism for the formation derivatives **5** or **6** *via* path a and path b, respectively is depicted in **Scheme-III**. TLC examination of the obtained product in different solvents showed a single spot indicating either **5** is formed or its regioisomer **6** is formed. IR spectrum of compound **5** or **6** showed bands at 1669 and 1636 cm^{-1} due to C=O and C=N functionalities. ^{1}H NMR spectrum of product **5** or **6** exhibited two signals of three protons each at δ 2.31 and δ 2.32 ppm, which are assigned to -CH_3 and -$COCH_3$ protons. Appearance of a signal of one proton at δ 5.61 ppm was ascribed to methine proton H_A. The signal for carbonyl carbon appeared at δ 189.4 ppm in the ^{13}C NMR spectrum of product **5** or **6**. Mass spectrum of the obtained product exhibited molecular ion peak at *m/z* 372 [M^+, 15%) and fragment ion peak at *m/z* 295 [M^+-C_6H_5, 100%] as base peak. IR and Mass spectra were of little help in deciding in favour of structure **5** or **6**. ^{1}H NMR spectrum of **5a** will exhibit the downfield shift of sandwich methyl group due to the anisotropic effect of carbonyl group on one side and phenyl ring on other side. In structure **6a**, phenyl group is away from methyl group and will exert little effect on its chemical shift. This fact only can distinguish between two structures **5a/6a** of the obtained product and on this basis structure **5a** is assigned which is validated by the DFT studies in the next section.

DFT studies of thiazolo[2,3-*b*]quinazoline 5a and its regioisomer 6a: The molecular geometry optimisation, IR, ^{1}H & ^{13}C NMR spectra calculations of thiazolo[2,3-*b*]quinazoline **5a** and its regioisomer **6a** were computed with Spartan 24 software package using B3LYP method [28-30] and employying 6-31G* basis set. The optimised structures of **5a** and **6a** are shown in Fig. 1. From the calculated energies, it is clearly indicated that both the regioisomers have nearly the similar energy but unexpectedly energy of **6a** is slightly lower than that of **5a** which has close proximity of methyl, acyl and

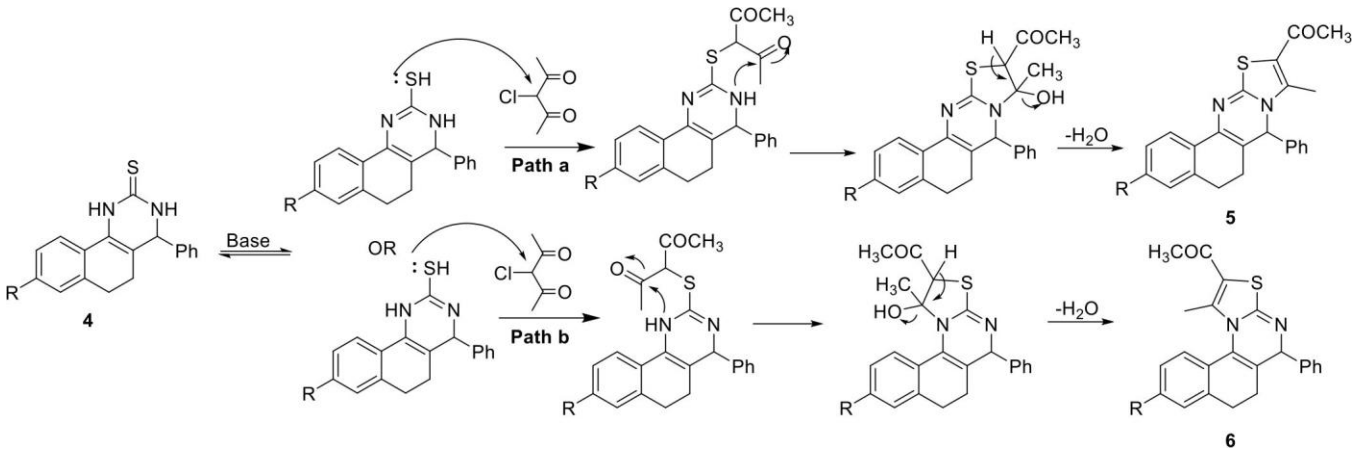

Scheme-III: Plausibe mechanism of formation of thiazole **5** or **6** from thione **4**

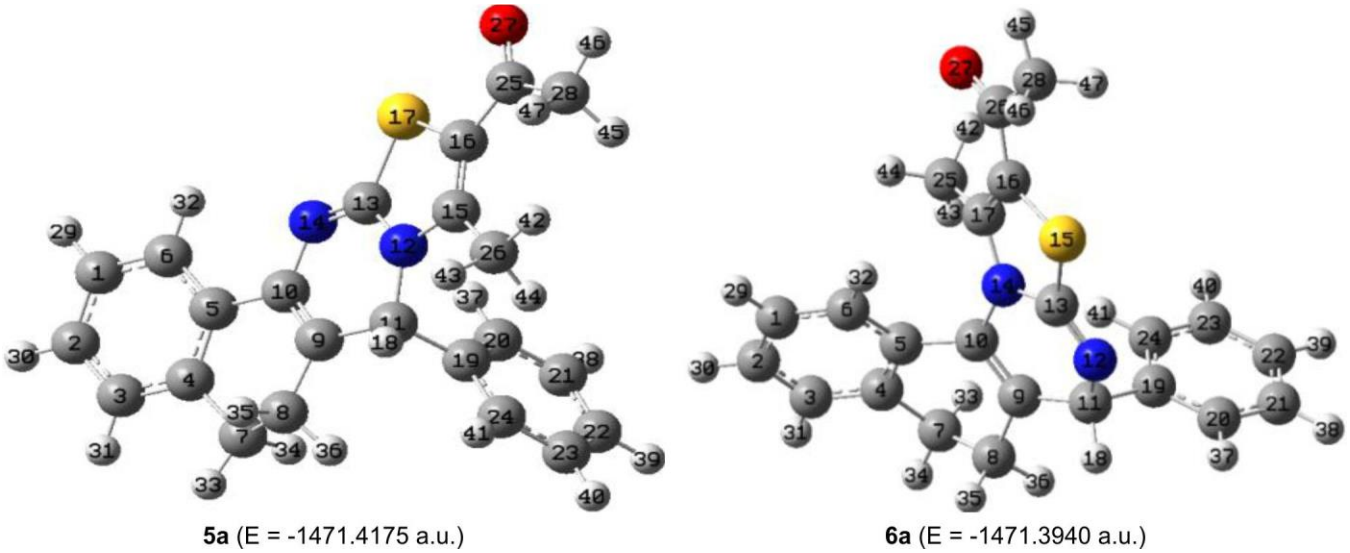

Fig. 1. Optimised structures of regioisomers **5a** and **6a**

phenyl groups. The difference in energy may be due to reason that calculations are performed in the gas phase.

^{1}H and ^{13}C NMR spectra of regioisomers **5a** and **6a** were computed by GIAO approach [31,32] with using B3LYP method and correlated with the experimental spectra (Fig. 2). ^{1}H and ^{13}C NMR chemical shifts (ppm) of compounds **5a** and **6a** have been recorded in Tables 1 and 2, respectively. The theoretical ^{1}H NMR spectra of **5a** and **6a** showed the methyl signal at δ 2.31 and 1.89 ppm, respectively. This downfield shift of methyl signal in compound **5a** is due to its deshielding by the carbonyl part of adjacent acyl group in **5a** on one side and phenyl group on the other side. In contrast, the influence of anisotropic effect by the phenyl group is absent in structure **6a**. The experimental chemical shift of methyl protons is observed downfield at δ 2.31 ppm, which supports assignment of structure **5a**. The correlation data of proton chemical shifts are found to be 0.99498 for structure **5a** and 0.99452 for regioisomer **6a** (Fig. 2). Similarly, the correlation figures of carbon chemical shifts of compounds **5a** and **6a** are com-

TABLE-1
COMPARISON DATA OF EXPERIMENTAL AND THEORETICAL ^{1}H NMR CHEMICAL SHIFTS

Protons	^{1}H NMR chemical shifts (ppm)		
	Exp	**5a** (DFT)	**6a** (DFT)
H-33 (C**H$_2$**)	2.08	1.68	1.44
COC**H$_3$**	2.31	2.03	2.14
H-35 (C**H$_2$**)	2.18	2.25	1.81
C**H$_3$**	2.32	2.31	1.89
H-33 (C**H$_2$**)	2.63	2.45	2.19
H-36 (C**H$_2$**)	2.80	2.56	2.65
H$_A$	5.61	5.09	5.37
H-31,32 (C$_6$H$_4$)	7.04	6.78	6.78
H-30 (C$_6$H$_4$)	7.15	6.99	6.80
H-29 (C$_6$H$_4$)	7.23	7.10	6.93
H-39 (C$_6$H$_5$)	7.30	7.23	7.04
H-38,40 (C$_6$H$_5$)	7.30	7.37	7.10
H-37,41 (C$_6$H$_5$)	7.90	7.86	7.16

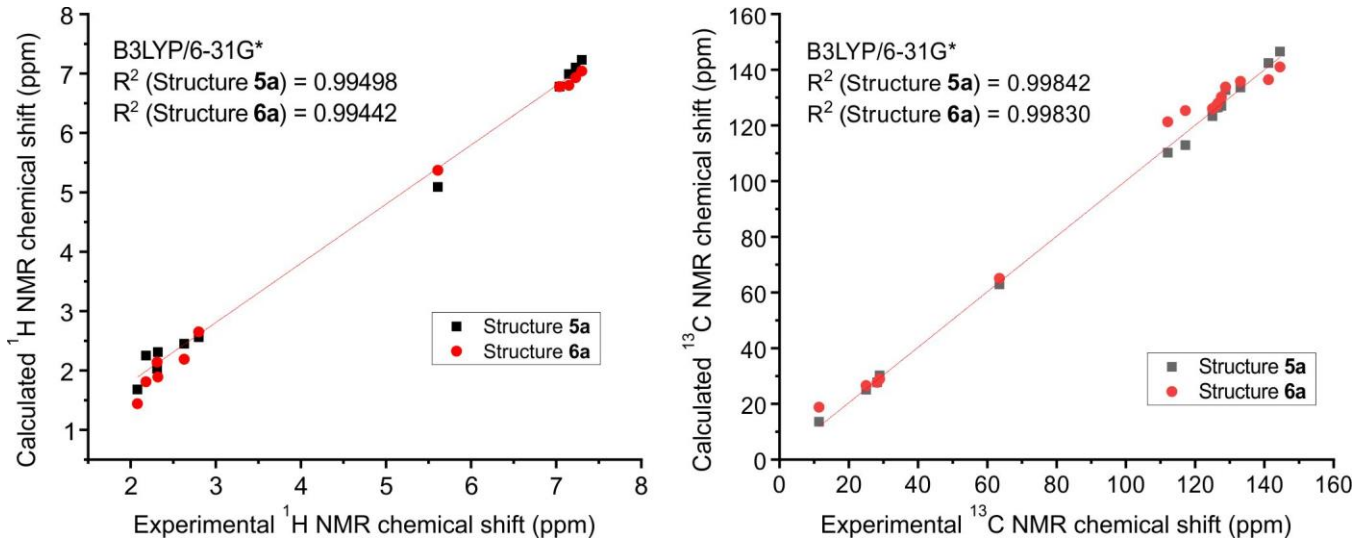

Fig. 2. Correlation of experimental ^{1}H & ^{13}C NMR spectra of **5a** with theoretical spectra of **5a** and regioisomer **6a**

TABLE-2
COMPARISON DATA OF EXPERIMENTAL AND THEORETICAL ^{13}C NMR CHEMICAL SHIFTS

Carbons	^{13}C NMR chemical shifts (ppm)		
	Exp	**5a**	**6a**
CH_3	11.4	13.6	18.8
CH_2	25	25.1	26.6
CO**C**H_3	28.2	27.7	27.7
CH_2	28.9	30.2	28.9
C-H_A	63.5	62.9	65.1
C-9	112.1	110.2	121.3
C-10	117.2	112.9	125.3
C-2, C-5	125	123.3	126
C-1, C-3	126.1	126.4	127
C-4, C-6	126.6	126.5	128
C-24, C-28	127.6	127	130.2
C-21, C-23	128.8	132.7	133.8
C-22, C-28	133.1	133.6	135.8
C-5, C-18	141.2	142.4	136.4
C-13, C-16	144.5	146.5	141

puted as 0.99842 and 0.9983, respectively (Fig. 2). The theoretical and experimental ^1H and ^{13}C NMR data shows rational correlations with the experimental data and validate the proposed structure **5a**.

The experimental IR spectrum of **5a** or **6a** exhibited C=O and C=C stretching bands at 1669 and 1586 cm^{-1}. Calculated IR spectra of **5a** and **6a** displayed C=O bands at 1663 and 1645 cm^{-1}, respectively. Calculated frequency of C=C bands in **5a** and **6a** are 1567 and 1534 cm^{-1}, respectively. The comparison of vibrational frequencies clearly reinforces assigned structure **5a.**

The HOMO-LUMO orbital diagram of **5a** and regioisomer **6a** is depicted in Fig. 3. The energy difference between HOMO-LUMO of both the regioisomers is 3.5 eV and 3.8 eV, respectively which shows **6a** is slightly more stable. The energy calculations also have the similar prediction. HOMO of **5a** shows the electron density is more concentrated on pyrimidine ring as compared to thiazole ring but reverse is true for LUMO. The electron density in HOMO of **6a** is more concentrated on thiazole ring as compared to pyrimidine ring. In LUMO, it is uniformally distributed on both thiazole and pyrimidine ring. Higher stability predictions for **6a** from energy as well as from HOMO-LUMO energy difference is attributed to calculations in the gas phase but due to various covalent and non-covalent interactions in the solid state, whereas **5a** exist as stable entity and it is the exclusive product formed in the reaction.

Crystallographic study and structural description of compounds 3a: Suitable crystal for diffraction studies of thiazole-4-carboxylate **3a** was recovered from dilute ethanol solution by slow evaporation method. X-ray diffraction measurements were performed on X Calibur EOS OXFORD diffractometer at 293 ± 2 K. Monochromatic Mo*K*α radiation (λ = 0.71073 Å) was used for collection of intensity data. SHELX-97 software package [33] was used to resolve the structure which is refined by full-matrix least-squares procedures on F^2. All non-hydrogen atoms were evolved with anisotropic thermal parameters.

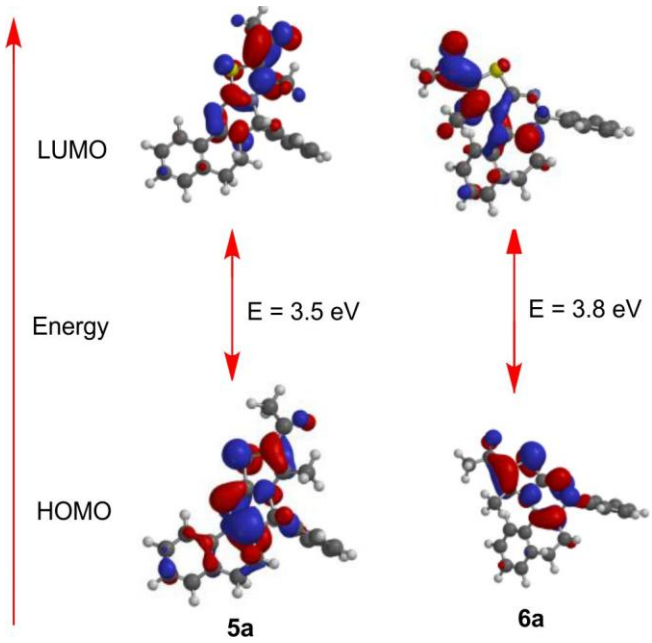

Fig. 3. HOMO-LUMO orbitals of **5a** and its regioisomer **6a**

Compound **3a** crystallizes in the triclinic system equipped with $P\bar{1}$ space group and the unit cell parameters are a = 14.275(5) Å, b = 7.558(4) Å, c = 16.416(6) Å, α = 90º, β = 102.78(4)º, γ = 90º. Parameters related to structure refinement of compound **3a** are compiled in Table-3. Some significant bond lengths and bond angles of **3a** are listed in Table-4. In the solid state, the C1-N1 and C12-N3 bond distances of

TABLE-3
STRUCTURE REFINEMENT PARAMETERS AND CRYSTAL DATA OF COMPOUND **3a**

CCDC no.	1037967
Empirical formula	$C_{16}H_{19.8}BrN_3O_2S$
Formula weight	398.07
Temperature (K)	293 (2)
Wavelength (Å)	0.71073 Å
Crystal system	Triclinic
Space group	P 1
Unit cell dimensions	
a (Å)	14.275(5)
b (Å)	7.558(4)
c (Å)	16.416(6)
α (º)	90.00
β (º)	102.78(4)
γ (º)	90.00
Volume ($Å^3$)	1727.4(12)
Z	4
Density (calculated) (Mg/m^3)	1.531 Mg/m^3
Absorption coefficient (mm^{-1})	2.513 mm^{-1}
Crystal size	–
Theta range for data collection	3.07 to 29.25
Reflections collected	1,122
Independent reflections	3,946
Data/restraints/parameters	3946/0/215
Goodness-of-fit on F^2	1.043
Final R indices [I>2σ(I) =2591 data]	R_1 = 0.1471, wR_2 = 0.3342
R indices (all data)	R_1 = 0.3386, wR_2 = 0.4355
Largest diff. Peak and hole (e $Å^{-3}$)	-0.629, 0.924

TABLE-4
SELECTED BOND PARAMETERS OF COMPOUND **3a**

Entry	Bond length (Å)	Entry	Bond angle (º)
S(1)–C(14)	1.768(16)	C(12)–S(1)–C(14)	88.5(7)
N(1)–C(1)	1.366(18)	C(1)–N(1)–N(2)	113.5(12)
N(1)–N(2)	1.420(16)	C(4)–C(3)–C(1)	112.9(15)
N(2)–C(12)	1.334(19)	C(12)–N(3)–C(13)	111.9(14)
N(3)–C(12)	1.335(18)	C(12)–N(2)–N(1)	114.0(12)
C(3)–C(4)	1.471(18)	C(3)–C(4)–C(5)	108.6(13)
N(3)–C(13)	1.39(2)	C(8)–C(7)–C(6)	124(2)
C(3)–C(1)	1.49(2)	C(11)–C(10)–C(9)	121.3(17)
C(8)–C(9)	1.39(3)	C(3)–C(1)–N(1)	126.0(14)
		N(3)–C(12)–N(2)	120.5(15)

1.366(18) Å and 1.335(18) Å, respectively, indicate the double bond nature of these bonds. The bond angles N3-C12-N2 and C11-C10-C9 are 120.5(15)º and 121.3(17)º respectively, which are consonant with the sp^2 hybrid nature of C-12 and C-10 atoms. The ORTEP diagram extracted from the X-ray structure of **3a** is shown in (Fig. 4). In the ORTEP diagram, the asymmetric unit of **3a** contains one HBr molecule included in the crystal lattice by hydrogen bonds between Br···N2 and Br···N3 (thiazole ring) with bond distance of 3.233 and 3.271 Å, respectively (Fig. 5). Ethyl group of this crystal is disordered and carbon atoms have been refined at two sites. The supramolecular assembly is stabilised by C–H···π interactions involving the contact C14–H14 and the centroid of aromatic ring of tetrahydronaphthalene moiety C_6H_6 (H14···g1 = 4.331 Å). Another short contact (C–H···π) is between N2-H and centroid of benzene ring (N2-H···g1 = 4.681) (Fig. 5). Very weak π-π stacking between the naphthalene moiety is observed (8.7 Å).

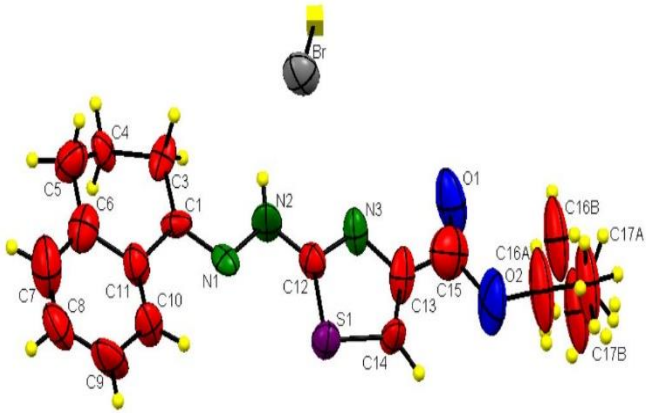

Fig. 4. ORTEP drawing indicating molecular structure and atomic labeling of (*E*)-ethyl 2-(2-(3,4-dihydronaphthalen-1(2*H*)-ylidene)hydrazinyl)-thiazole-4-carboxylate (**3a**)

Antimicrobial studies: Disc diffusion method [34,35]. was employed to assay the *in vitro* antibacterial activities of compounds **3** and **5** against *S. aureus* and *E. coli* bacterial strains. Dimethyl sulfoxide and meropenem antibiotic were utilised as blank and standard, respectively. A 125 µg/mL concentration was used to perform experiments in triplicate and average results of measurement of zone of inhibition (mm) are depicted as mean ± standard deviation. Minimum inhibitory concentration (MIC) of tested compounds in µg/mL was analysed in the range of 6.25-150 µg/mL. Thiazole-4-carboxylate derivatives **3a** and **3b** shows moderate activity against *E. coli* and *S. aureus*, respectively. Quinazoline-thiazole **5a** exhibits good inhibition (MIC 25 and 50 µg/mL) of both strains as compared to the moderate activity of **5b** (Table-5).

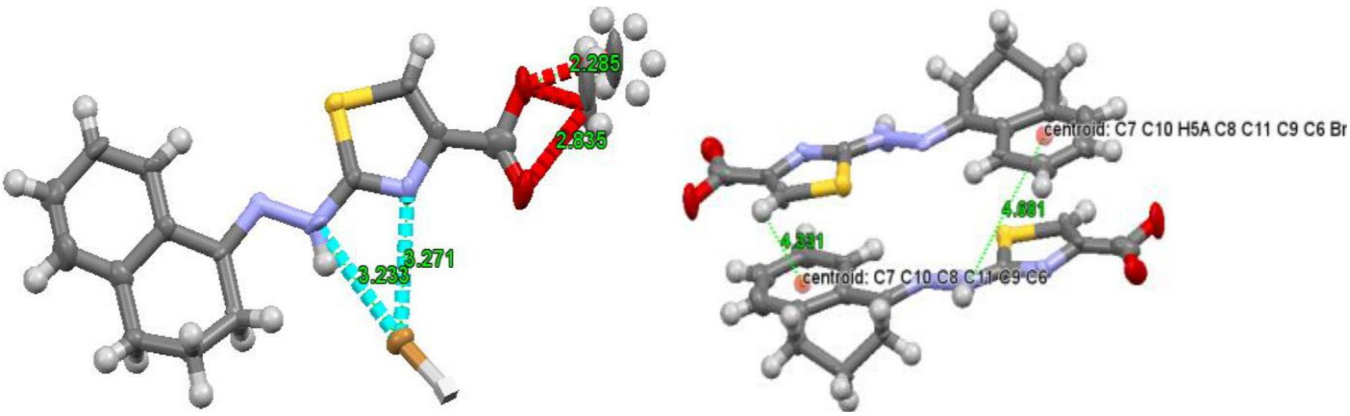

Fig. 5. Hydrogen bonds and supramolecular interactions in thiazole-4-carboxylate (**3a**)

TABLE-5
ANTIBACTERIAL ACTIVITY DATA OF COMPOUNDS **3** AND **5**

Entry	Compound	Zone of inhibition (mm)		MIC (µg/mL)	
		S. aureus	*E. coli*	*S. aureus*	*E. coli*
1	**3a**	14 ± 0.41*	16 ± 0.41	75	62.5
2	**3b**	12 ± 1.20	11 ± 0.82	100	125
3	**5a**	24 ± 0.82	18 ± 0.41	12.5	25
4	**5b**	18 ± 0.41	16 ± 0.82	25	50
	Meropenem (std. antibiotic)	31 ± 0.41	22 ± 1.20	6.25	6.25
	DMSO	00	00	00	00

*Mean ± standard deviation

Conclusion

This work reports the ultrasound assisted synthesis of naphthalenyl-hydrazinyl- and quinazolinyl-thiazole derivatives in quantitative yields. The structure of new compounds has been established by spectral techniques. X-ray diffraction studies of hydrazinyl-thiazole-4-carboxylate **3a** were undertaken to gain insight in to the supramolecular interactions in crystalline state. Spectral data computed from DFT studies on Spartan software package provided structural distinction between the two regioisomers. Antibacterial studies of new compounds have shown that all the compounds are moderately active against *S. aureus* and *E. coli* bacterial strains.

Supplementary information: The crystallographic information file of compound **3a** is deposited with the Cambridge Structural Database Centre and can be obtained *via* www.ccdc.cam.ac.uk/data_request/cif

CONFLICT OF INTEREST

The authors declare that there is no conflict of interests regarding the publication of this article.

DECLARATION OF AI-ASSISTED TECHNOLOGIES

During the preparation of this manuscript, the authors used an AI-assisted tool(s) to improve the language. The authors reviewed and edited the content and take full responsibility for the published work.

REFERENCES

1. N. Bhanwala, V. Gupta, L. Chandrakar and G.L. Khatik, *ChemistrySelect*, **8**, e202302803 (2023); https://doi.org/10.1002/slct.202302803
2. M.F. Arshad, A. Alam, A.A. Alshammari, M.B. Alhazza, I.M. Alzimam, M.A. Alam, G. Mustafa, M.S. Ansari, A.M. Alotaibi, A.A. Alotaibi, S. Kumar, S.M.B. Asdaq, M. Imran, P.K. Deb, K.N. Venugopala and S. Jomah, *Molecules*, **27**, 3994 (2022); https://doi.org/10.3390/molecules27133994
3. M. Gümüş, M. Yakan and İ. Koca, *Future Med. Chem.*, **11**, 1979 (2019); https://doi.org/10.4155/fmc-2018-0196
4. A. Singh, D. Malhotra, K. Singh, R. Chadha and P.M.S. Bedi, *J. Mol. Struct.*, **1266**, 133479 (2022); https://doi.org/10.1016/j.molstruc.2022.133479
5. P. Kushwaha and S. Pandey, *Antiinflamm. Antiallergy Agents Med. Chem.*, **22**, 133 (2023); https://doi.org/10.2174/0118715230276678231102150158
6. A.F. Kassem, R.H. Althomali, M.M. Anwar and W.I. El-Sofany, *J. Mol. Struct.*, **1303**, 137510 (2024); https://doi.org/10.1016/j.molstruc.2024.137510
7. P. Venkatesham, D. Schols, L. Persoons, S. Claes, A.A. Sangolkar, R. Chedupaka and R.R. Vedula, *J. Mol. Struct.*, **1286**, 135573 (2023); https://doi.org/10.1016/j.molstruc.2023.135573
8. J. Guo, Z. Xie, W. Ruan, Q. Tang, D. Qiao and W. Zhu, *Eur. J. Med. Chem.*, **259**, 115689 (2023); https://doi.org/10.1016/j.ejmech.2023.115689
9. Y. Li, N. Sun, H.-L. Ser, W. Long, Y. Li, C. Chen, B. Zheng, X. Huang, Z. Liu and Y.-J. Lu, *RSC Adv.*, **10**, 15000 (2020); https://doi.org/10.1039/D0RA00691B
10. S.K. Bharti, G. Nath, R. Tilak and S.K. Singh, *Eur. J. Med. Chem.*, **45**, 651 (2010); https://doi.org/10.1016/j.ejmech.2009.11.008
11. U. Debnath, K.K. Roy and A. Kumar, *Synlett*, **36**, 2705 (2025); https://doi.org/10.1055/a-2637-7462
12. K.H. Narasimhamurthy, T.R. Swaroop and K.S. Rangappa, *Eur. J. Med. Chem. Rep.*, **12**, 100225 (2024); https://doi.org/10.1016/j.ejmcr.2024.100225
13. V. Martínez-Rosas, B. Hernández-Ochoa, L. Morales-Luna, D. Ortega-Cuellar, A. González-Valdez, R. Arreguin-Espinosa, Y. Rufino-González, E. Calderón-Jaimes, R.A. Castillo-Rodríguez and S. Gómez-Manzo, *Int. J. Mol. Sci.*, **24**, 11516 (2023); https://doi.org/10.3390/ijms241411516
14. Z.-X. Niu, Y.-T. Wang, S.-N. Zhang, Y. Li, X.-B. Chen, S.-Q. Wang, and H.-M. Liu, *Eur. J. Med. Chem.*, **250**, 115172 (2023); https://doi.org/10.1016/j.ejmech.2023.115172
15. P.C. Sharma, K.K. Bansal, A. Sharma, D. Sharma and A. Deep, *Eur. J. Med. Chem.*, **188**, 112016 (2020); https://doi.org/10.1016/j.ejmech.2019.112016
16. R.P. Karuvalam, K.R. Haridas, S.K. Nayak, T.N.G. Row, P. Rajeesh, R. Rishikesan and N.S. Kumari, *Eur. J. Med. Chem.*, **49**, 172 (2012); https://doi.org/10.1016/j.ejmech.2012.01.008
17. J. Bueno, M.M. Carda, B. Crespo, A.C. Cuñat, C. de Cózar, M.L. León, J.A. Marco, N. Roda and J.F. Sanz-Cervera, *Bioorg. Med. Chem. Lett.*, **26**, 3938 (2016); https://doi.org/10.1016/j.bmcl.2016.07.010
18. M. El-Shahat, N. Tawfek and W.I. El-Sofany, *Chem. Biodivers.*, **2040**, 202402042 (2024); https://doi.org/10.1002/cbdv.202402042
19. F.A. Al-Omary, G.S. Hassan, S.M. El-Messery and H.I. El-Subbagh, *Eur. J. Med. Chem.*, **47**, 65 (2012); https://doi.org/10.1016/j.ejmech.2011.10.023
20. A. Şandor, I. Fizeşan, I. Ionuț, G. Marc, C. Moldovan, I. Oniga, A. Pîrnău, L. Vlase, A.-E. Petru, I. Macasoi and O. Oniga, *Biomolecules*, **14**, 218 (2024); https://doi.org/10.3390/biom14020218.
21. D. Panigrahi and S.K. Sahu, *BMC Chem.*, **19**, 39 (2025); https://doi.org/10.1186/s13065-024-01357-2
22. C. Hillel, S. Collins, A. Parihar, O. Mermut, C.J. Barrett, W.J. Pietro and L. Reven, *Phys. Chem. Chem. Phys.*, **27**, 5228 (2025); https://doi.org/10.1039/D4CP04159C
23. D. Majumdar, J.E. Philip, S. Roy, B. Gassoumi and H. Ghalla, *BMC Chem.*, **19**, 227 (2025); https://doi.org/10.1186/s13065-025-01570-7
24. H. Guan, H. Sun and X. Zhao, *Int. J. Mol. Sci.*, **26**, 3262 (2025); https://doi.org/10.3390/ijms26073262
25. P. Sharma, P. Ranjan and T. Chakraborty, *Mol. Phys.*, **122**, (2024); https://doi.org/10.1080/00268976.2024.2331620
26. D. Gautam, P. Gautam and R.P. Chaudhary, *Heterocycl. Commun.*, **17**, 147 (2011); https://doi.org/10.1515/hc.2011.027
27. R. Gupta and R.P. Chaudhary, *Asian J. Chem.*, **24**, 2113 (2012).
28. A.D. Becke, *Phys. Rev. A Gen. Phys.*, **38**, 3098 (1988); https://doi.org/10.1103/PhysRevA.38.3098
29. C. Lee, W. Yang and R.G. Parr, *Phys. Rev. B Condens. Matter*, **37**, 785 (1988); https://doi.org/10.1103/PhysRevB.37.785
30. J. Tomasi, B. Mennucci and E.J. Cances, *J. Mol. Struct. THEOCHEM*, **464**, 211 (1999); https://doi.org/10.1016/S0166-1280(98)00553-3
31. J. Tomasi and M. Persico, *Chem. Rev.*, **94**, 2027 (1994); https://doi.org/10.1021/cr00031a013
32. R. Ditchfield, *J. Chem. Phys.*, **65**, 3123 (1976); https://doi.org/10.1063/1.433526
33. G.M. Sheldrick, SHELX-97, Program for Refinement of Crystal Structure, University of Gottingen, Gottingen, Germany (1997).
34. J.H. Jorgensen, J.D. Turnidge, J.A. Washington, P.R. Murray, M A. Pfaller, F.C. Tenover, E.J. Baron and R.H. Yolken, in eds.: P.R. Murray, E.J. Baron, M.A. Pfaller, F.C. Tenover and R.H. Yolken, Antibacterial Susceptibility Tests: Dilution and Disk Diffusion Methods; In: Manual of Clinical Microbiology, Washington, DC, USA: ASM Press, edn. 7, pp. 1526-1543 (1999).
35. B.A. Arthington-Skaggs, M. Motley, D.W. Warnock and C.J. Morrison, *J. Clin. Microbiol.*, **38**, 2254 (2000); https://doi.org/10.1128/JCM.38.6.2254-2260.2000